MAXIMUM LIKELIHOOD ESTIMATION OF ARRAY ELEMENT LOCATION AND MVDR BEAMFORMING : SIMULATION AND EXPERIMENTAL RESULTS

Larry K. Lam   Theagenis J. Abatzoglou

e-mail : Lam_larry.mm.rdd.LMSC.Lockheed.com
Lockheed Research and Development Division (O/97-80, B/251)
Lockheed Missiles and Space Co. Palo Alto, California, 94304

Abstract

A Maximum Likelihood Array Element Location (ML-AEL) algorithm was developed for estimating the relative AEL of a sonar array in 3 dimensions. The information was used after the array deployment to improve the performance of an adaptive beamformer. The algorithm minimizes an objective function over the estimated AEL, and parameters pertaining to plane waves incident on the array from unknown directions and multipaths. Results obtained from computer simulated and experimental data are presented. The performance of the algorithm applied to experimental data was evaluated using an enhanced version of the adaptive beamforming algorithm called Minimum Variance Distortionless Response (MVDR).

1. Introduction

The underwater ambient noise environment is highly non-uniform in the spatial and temporal domains. On the other hand, the digitization of the outputs of a sonar array has permited the application of advanced adaptive array signal processing algorithm to extract weak signals amid environmental noise and strong interfering signals. Adaptive algorithms such as the Minimum Variance Distortionless Response (MVDR), have been shown to achieve considerable lower sidelobe levels in arbitrary configured discrete arrays than conventional beamformer, but the effectiveness of these algorithms can be severely degraded by sensor location errors. This paper reports on the experiment whose aim is to reduce these errors.

Weiss and Friedlander [1] has described an iterative technique to estimate the locations of sensors using sources at unknown locations. Following their work, we have developed a Maximum Likelihood Array Element Locations (ML-AEL) estimator for estimating the relative locations of the elements of a sonar array in 3 dimensions. The estimator is based on the snapshots of the array output for plane wave incidences from unknown directions and multipaths.

Although a specific array configuration is assumed in the paper, the technique described in the following is applicable to more general configurations.

2. Problem Formulation

Consider an arbitrary sonar array of M elements located at $w_m = (x_m, y_m, z_m)$, $m = 1, \ldots, M$, but they are not known to the observer. The array snapshots are denoted by

$$\vec{x}_{n,p} = \left[\cdots \; exp\left(-j\frac{2\pi}{\lambda} W\vec{u}\left(\theta_{q(p)}, \phi_{q(p)}\right)\right) \; \cdots\right]\vec{a}_{n,p} + \vec{v}_{n,p} \qquad (1)$$

$$W = \begin{bmatrix} w_1 \\ \vdots \\ w_M \end{bmatrix}, \quad \vec{u}(\theta,\phi) = (\cos\phi\sin\theta, \cos\phi\cos\theta, \sin\phi)^T$$

where λ is the wavelength, and the subscripts denote the n^{th} snapshot, p^{th} source, and q^{th} propagation path, $\vec{a}_{n,p}$ describe the signal amplitudes, $\vec{v}_{n,p}$ is the array noise.

The array manifold matrix

$$\left[\cdots \; \exp\left(-j\frac{2\pi}{\lambda} W\vec{u}\left(\theta_{q(p)}, \phi_{q(p)}\right)\right) \; \cdots\right]$$

contains the path delay information for the incident plane waves.

The Maximum Likelihood estimator for sensor locations is obtained by minimizing the objective function

$$G = \sum_{p=1}^{P}\left(\vec{x}_{n,p} - \vec{s}\left(\vec{\theta}_p, \vec{\phi}_p, \vec{a}_{n,p}, \vec{w}\right)\right)^* R_p^{-1}\left(\vec{x}_{n,p} - \vec{s}\left(\vec{\theta}_p, \vec{\phi}_p, \vec{a}_{n,p}, \vec{w}\right)\right)$$

$$\vec{s}\left(\vec{\theta}_p, \vec{\phi}_p, \vec{a}_{n,p}, \vec{w}\right) = \left[\cdots \; \exp\left(-j\frac{2\pi}{\lambda} W\vec{u}\left(\theta_{q(p)}, \phi_{q(p)}\right)\right) \; \cdots\right]\vec{a}_{n,p}$$

for p = 1, ... P. (2)

The spatial array noise correlation matrix, R_p, is

$$R_p = \sum_{n=1}^{N} \vec{v}_{n,p}\vec{v}_{n,p}^{\;*} \qquad (3)$$

The objective function is also expressed as

$$G = \sum_{p=1}^{P} G_p$$

$$G_p = \left(\vec{x}_{n,p} - \vec{s}\left(\vec{\theta}_p, \vec{\phi}_p, \vec{a}_{n,p}, \vec{w}\right)\right)^* R_p^{-1} \left(\vec{x}_{n,p} - \vec{s}\left(\vec{\theta}_p, \vec{\phi}_p, \vec{a}_{n,p}, \vec{w}\right)\right)$$

This function is minimized iteratively over the estimated AEL $\vec{w}$ and the parameters $\vec{\theta}_p, \vec{\phi}_p, \vec{a}_{n,p}$, which specify the sources and their propagation paths. To simplified the above expressions, we assumed narrow band CW sources, thus $\vec{a}_{n,p} = \exp(2\pi jnfT)\vec{a}_p$. By dropping the $\exp(2\pi jnfT)$ term the expression in (3) yields

$$\vec{s}\left(\vec{\theta}_p, \vec{\phi}_p, \vec{a}_p, \vec{w}\right) = \left[\cdots \quad \exp\left(-j\frac{2\pi}{\lambda} W\vec{u}\left(\theta_{q(p)}, \phi_{q(p)}\right)\right) \quad \cdots\right]\vec{a}_p \tag{4}$$

This is equivalent to taking a block of snapshot data and collapsing it into a vector along the time dimension, which makes for more efficient computation.

The coordinate system is defined in accordance to the Navy convention. The x axis points to the East, y axis North, and z axis up. The azimuthal angle θ is the angle clockwise from the North, the elevation angle ϕ is the angle measured from the horizontal plane. The center of the array is the origin.

2. The Minimization Procedure

The first step is to estimate the parameters of the amplitudes and angles of arrival (AOA), $\vec{\theta}_p, \vec{\phi}_p, \vec{a}_{n,p}$, of the incident plane waves. This is done by minimizing G iterative over these parameters holding the element locations constant. The signal model is that of a direct path and a multipath signls, plane wave incidences on the array from a single source, which illuminates the array from P distinct AOA. The rough estimates of $\vec{\theta}_p, \vec{\phi}_p, \vec{a}_{n,p}$ are obtained by conventional bemforming using the best available estimates of element positions. More precise estimates are obtained by applying the Newton method for minimizing a function of several variables to find the minimum of the objective function G. To estimate the parameters for the pth source it suffices to minimize G_p. This follows the approach in [1].

The second step is to minimize the overall objective function *G* by adjusting the element locations holding the sources parameters constant. This step is simplified substantially if the noise correlation matrix is diagonal. Then the minimization can be done with respect to the AEL of the hydrophones individually. The second step is also based on the Newton method. Steps 1 and 2 are repeated until the estimated AEL converge.

3. The Simulation

A computer simulation was developed to support a sea trial which was to demonstrate an advance passive sonar array. A task was to calibrate the array using the ML-AEL algorithm. The array had five arms, with 10 hydrophones affixed to each arm at the radial distances of 3, 6, 9, 12, 15, 21, 27, 33, 56, and 80 feet. The five arms were connected at one end. When deployed, they extended radially outward at angular separation of 72 degrees. Due to the flexibility of the structure, the separation of the arms could vary by a few degrees in azimuth and a lot more in elevation.

A set of simulated element locations was generated by adding random deviations to a set of nominal AEL. The variance of the deviation was made larger for the outer hydrophones. For example, a hydrophone at the 3 feet radial distance could be deviated by an inch, where the hydrophone at 80 feet could be deviated by 2 feet. A set of simulated array snapshot data was generated based on a set of parameters specified for the source locations and multipaths conditions.

The ML-AEL algorithm was applied to the simulated data, initialized using the nominal AEL. The estimated AEL were compared with the simulated AEL to determine the error. The following contained some of the findings that were helpful to preparing for the sea trial.

Although using sources that would be operated at a higher acoustic frequency, and that would be placed at more numerous locations to illuminate the array from distinct angular directions should produce more precise AEL estimates, the simulation results showed that these were not the most important factors. The two factors that mattered the most were SNR and the angular separation between the direct and multipath signals.

The signal to noise ratio used in the simulation was varied from 15 to 30 dB, defined by the ratio of the direct path signal to the noise. The Hessian matrix in the Taylor series expansion used in the Newton method was positive definite for SNR above 10 dB. Below that, the Hessian became negative frequently, resulting in long iteration time and large errors.

Figure 3.1 illustrates the RMSE of the estimated AEL based on 5 simulation runs for SNR = 20, 25, 30 dB. The array was illuminated successively from 5 distinct directions using a 600 Hz CW. The RMSE was less than half an inch for SNR = 30 dB. This level of error was approximately 0.005 wavelength in water. Thus, the phase and amplitude response of the array electronics were calibrated to an uncertainty of less than 2 degrees and 0.1 dB respectively.

The ML-AEL algorithm assumed a data model consisting of two plane waves arriving at the array, corresponding to the direct path and multipath signals. When the multipath was well separated from the direct path in angle of arrival, step 1 of the ML-AEL procedure converged quickly. Otherwise, the errors in the estimated angles of arrival and signal amplitudes may induced large AEL errors in step 2.

In simulation, a single multipath was assigned to an acoustic source, which was assumed to be 6 feet below a flat reflective sea surface. A reflection coefficient of -1 was assumed at the water/air interface. The direct path signal was the sum of the signal from the source and its image. The multipath signal was the signal from the source reflected from the sea floor and sea surface (ref fig 4.1). This geometry was selected to separate the multipath from the direct path.

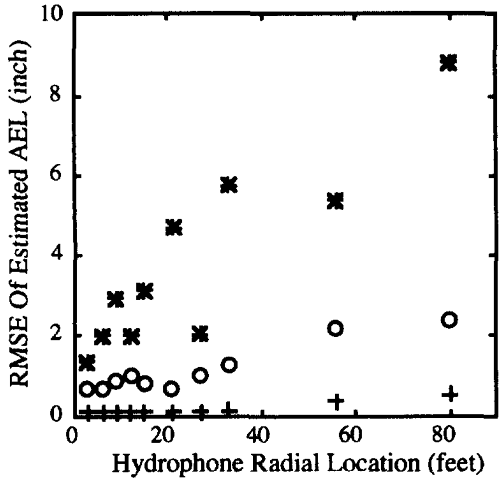

Figure 3.1 **The RMSE of the estimated locations vs. the radial locations of the hydrophones, for various SNR, “*” 20, “o” 25, “+” 30 dB.**

4. The Experiment

It was important to develop a simulation to model the underwater environment properly, just as it was important to develop a set of experimental conditions that ensured the correctness of the data model assumed by the ML-AEL algorithm. The experiment is described in the following to provide for a proper interpretation of the results.

The array was deployed at a depth of 400 feet. A single acoustic source was used to illuminate the array. It was placed at six locations encompassing the array, nominally at 1500 feet from the array and 6 feet under the sea surface, as illustrated in figure 4.1. At each location, the source transmitted a sequence of CW pulses, 200 msec in duration, every 5 seconds, with the center frequency changing discretely from 500, to 600, to 700 Hz from pulse to pulse. The source output was adjusted to produce a signal to noise ratio of greater than 25 dB, monitored at the outputs of the array.

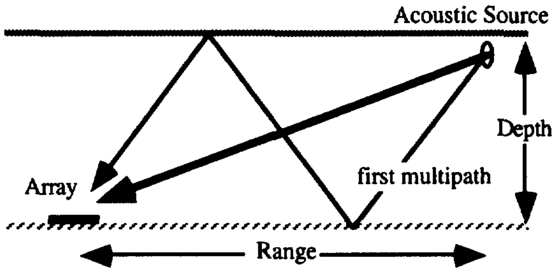

Figure 4.1 **The geometry for the experiment.**

The timing of the signals arriving at the array determined when to select the snapshot data at the output of the array. Setting t = 0 to define the arrival of the direct path signal, the first multipath signal arrived at t = 75 msec, and the second at 190 msec. Since it took 50 msec for the direct path signal to reach from one end of the array to the other, between the direct and first multipath signals was a temporal window of 30 msec. The next window was the 70 msec between the first and second multipath signals. The snapshot data was taken from the 70 msec window.

An example of the output data is shown in figure 4.2. The acoustic frequency was 600 Hz. The digitized data was down converted to baseband in software. Data snapshots were taken from a window centered at 2.9 sec.

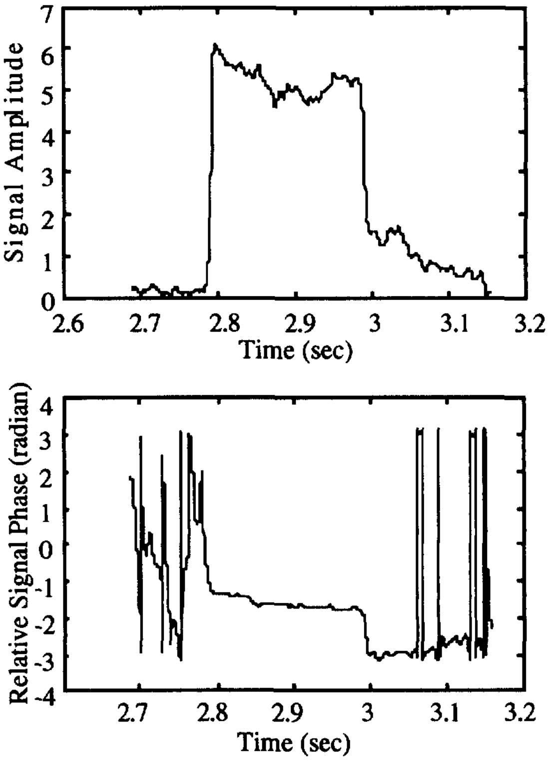

Figure 4.2 **The output of a typical hydrophone.**

The variations in the amplitude and phase of the signals suggested that there were more than one multipath signals. This had been expected. The outputs of the hydrophones near the perimeter of the array showed the arrivals of the multipath signals with discrete phase and amplitude changes. For those near the center of the array the phase and amplitude changes were convoluted. This suggested that local acoustic scattering near the array center was present. A potential source of local scattering was an enclosure for the electronics. It was located near the center of the array situated between arms 1 and 5 as shown in figure 4.3.

The ML-AEL minimization procedure was initialized with AEL values that had been measured immediately prior to deployment. The algorithm was applied to the experimental data in a different manner than in simulation, because the acoustic source was not in the far field of the array.

A subarray was defined by excluding the two outer hydrophones, so that the source was in the far field of the subarray. After the subarray AEL had been estimated, the locations of the outer phones were estimated individually by holding the subarray AEL constant.

Several sets of experimental data were processed, the algorithm generally converged to solutions that were slightly different depending on the data set used. In addition, the algorithm usually took three times longer than the corresponding simulation runs. A set of AEL estimates is illustrated in figure 4.3. The measured positions indicated by '+' were obtained prior to deployment. Only 41 of the 50 hydrophones were functional.

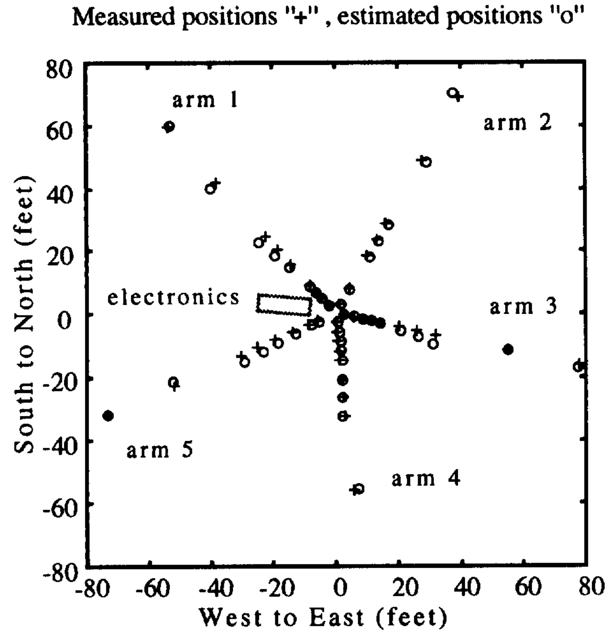

Figure 4.3 The measured vs estimated AEL.

Since it was not feasible to measure the true positions of the hydrophones post array deployment, the evaluation of the experimental results required an objective measure, which was selected to be the output of an adaptive beamformer. The interference suppression performance of the Minimum Variance Distortionless Response (MVDR) algorithm was sensitive to errors in AEL.

5. The Adaptive Beamformer

The MVDR and MUSIC algorithms have been designed for high resolution adaptive beamforming [2, 3]. They are especially efficient when the array has arbitrary geometry because then conventional beamforming usually produces high sidelobe levels while the sidelobes of the high resolution beamformers can be kept at an acceptable level.

We now describe the MVDR and enhanced MVDR algorithms. Consider the data snapshots $\vec{x}_n$, n = 1, ..., N, the array snapshot correlation matrix is defined by

$$R = \frac{1}{N}\sum_{n=1}^{N} \vec{x}_n \vec{x}_n^{\,*} . \tag{5}$$

In the presence of P uncorrelated narrowband sources or interferers, R can be approximately by

$$R = \sum_{p=1}^{P} |A_p|^2 \, \vec{e}(\theta_p,\phi_p)\vec{e}(\theta_p,\phi_p)^* + \sigma^2 I \tag{6}$$

where $|A_p|^2$, $\vec{e}(\theta_p,\phi_p)$ are the power and steering vector of the pth source or interferer at the incident angle (θ_p,ϕ_p) in azimuth and elevation, and σ^2 is the element variance of spatial white noise.

The MVDR is obtained for a selected angle by using a weight vector $\vec{\xi}$ that minimizes the overall spatial response, but that is constrained to produce a unit response at the selected angle, (θ,ϕ). This is expressed by

$$\underset{\xi}{Min}\left\{\vec{\xi}^* R \vec{\xi}\right\} \text{ subject to } \vec{\xi}^* \vec{e}(\theta,\phi) = 1 \tag{7}$$

The MVDR spatial spectrum is computed from

$$S_{MVDR}(\theta,\phi) = \frac{1}{\vec{e}(\theta,\phi)^* R^{-1} \vec{e}(\theta,\phi)} \tag{8}$$

To unravel the presence of closely spaced multipath signals, an enhanced MVDR was used to emphasize the signal structure present. Enough time integration in the computation of the correlation matrix was attained to allow some decorrelation of the multipath return from the direct path. The correlation matrix, R, can be approximated by the eigenvector-eigenvalue decomposition

$$R = E\Lambda E^* + \sigma^2 . \tag{9}$$

where $E = \left[\vec{E}_1 \cdots \vec{E}_q\right]$ is the set of signal orthonormal eigenvectors, and $\Lambda = diag\left(\lambda_1, \cdots, \lambda_q\right)$ is the set of eigenvalues in arranged in a descending order. The eigenvector-eigenvalues are selected based on an appropriate threshold level that has been selected to separate signal from noise. The resolution of the MVDR spatial spectrum is enhanced by emphasizing more of the signal characteristics estimated by $E\Lambda E^*$. The enhanced MVDR spatial spectrum is

$$S_{Enhanced\_MVDR}(\theta,\phi) = \frac{1}{\vec{e}(\theta,\phi)^*\left[R + \mu E\Lambda E^*\right]^{-1}\vec{e}(\theta,\phi)} \tag{10}$$

where μ is a parameter that controls the level of enhancement.

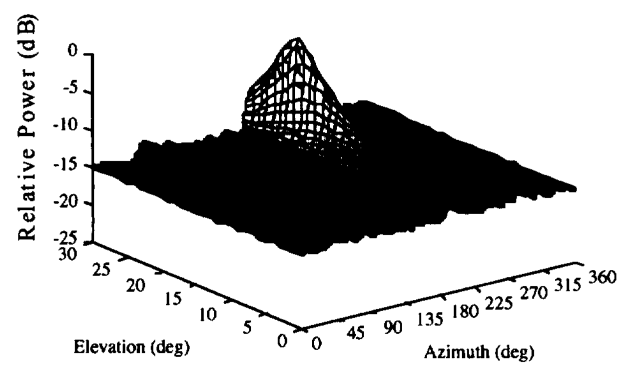

Figure 5.1. The enhanced MVDR spatial spectrum for a single source without AEL correction.

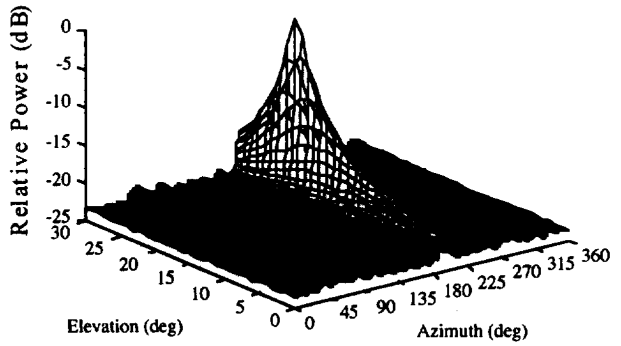

Figure 5.2. The enhanced MVDR spatial spectrum for a single source with AEL correction.

The enhanced MVDR spatial spectrum without and with AEL correction are shown in the figures 5.1 and 5.2 respectively. The sidelobe level was improved from – 15 to – 22 dB using the estimated AEL, a 7 dB improvement. The acoustic frequency of the source was 700 Hz.

The results shown in figures 5.1 and 5.2 were produced using the data collected by a subarray consisted of the first to the seventh inner hydrophones on arms 2, 3 and 4. The inclusion of the data from a larger array did not produce a spatial spectrum with sufficiently low sidelobes. The cause was still being investigated. Besides the AEL algorithm, there were a number of electronics, structural and environmental factors that may be contributing to this problem. One of them may be that effects of local acoustic scattering were not modeled. Another may be that the reflection properties of the sea floor were not spatially uniform.

6. Conclusion

A ML-AEL algorithm for estimating array element locations in 3D and with multipath was described. AEL results obtained from processing simulated and experimental data were presented. The ML-AEL algorithm was shown to be capable of producing a precise AEL estimate. An RMSE of less than an inch could be achieved for SNR greater than 30 dB. The performance of the ML-AEL algorithm against experimental data was evaluated using an enhanced version of the MVDR algorithm. The difference before and after AEL correction was shown to be an improvement of 7 dB, measured in terms of lower sidelobes levels of the MVDR spatial spectrum.

The results presented in the paper were tentative, and the experimental results obtained could be interpreted given the complexity of the underwater acoustic environment. The sea trial was successful in showing the merits of the ML-AEL algorithm and the performance of the array. The enhanced MVDR algorithm was instrumental to the evaluation of the experimental data.

There were at least two areas that needed improving. The collection of far field data for AEL correction was a time consuming task. The minimization procedure was not highly reliable because it may fail to converge. For these reasons, a near field AEL algorithm is being considered.

References

[1] A. T. Weiss and B. Friedlander, "Array Shape Calibration using Sources in Unknown Locations", IEEE Trans. Accost, Sp. and Sign. Proc., vol. 37, pp. 1958-1966, Dec, 1989.

[2] Haykin, E., "Array Signal Processing", Chapter 3, Prentice Hall, Inc., 1985, New Jersey.

[3] H. Cox, R. Zeshind and M . Owen, "Robust Adaptive Beamforming", IEEE Trans. Acoust, Sp. and Sign. Proc., vol. 35, pp. 1365-1376, Oct, 1987.